Atmospheric Chemistry of i-Butanol

ARTICLE *in* THE JOURNAL OF PHYSICAL CHEMISTRY A · NOVEMBER 2010

Impact Factor: 2.69 · DOI: 10.1021/jp107950d · Source: PubMed

Atmospheric Chemistry of *i*-Butanol

V. F. Andersen,[†] T. J. Wallington,*[,‡] and O. J. Nielsen[†]

Copenhagen Center for Atmospheric Research, Department of Chemistry, University of Copenhagen, Universitetsparken 5, DK-2100 Copenhagen, Denmark, and Systems Analytics and Environmental Sciences Department, Ford Motor Company, Mail Drop RIC-2122, Dearborn, Michigan 48121-2053, United States

Received: August 22, 2010; Revised Manuscript Received: October 21, 2010

Smog chamber/FTIR techniques were used to determine rate constants of $k(Cl + i\text{-butanol}) = (2.06 \pm 0.40) \times 10^{-10}$, $k(Cl + i\text{-butyraldehyde}) = (1.37 \pm 0.08) \times 10^{-10}$, and $k(OH + i\text{-butanol}) = (1.14 \pm 0.17) \times 10^{-11}$ cm^3 $molecule^{-1}$ s^{-1} in 700 Torr of N_2/O_2 diluent at 296 ± 2K. The UV irradiation of *i*-butanol/Cl_2/N_2 mixtures gave *i*-butyraldehyde in a molar yield of 53 ± 3%. The chlorine atom initiated oxidation of *i*-butanol in the *absence* of NO gave *i*-butyraldehyde in a molar yield of 48 ± 3%. The chlorine atom initiated oxidation of *i*-butanol in the *presence* of NO gave (molar yields): *i*-butyraldehyde (46 ± 3%), acetone (35 ± 3%), and formaldehyde (49 ± 3%). The OH radical initiated oxidation of *i*-butanol in the *presence* of NO gave acetone in a yield of 61 ± 4%. The reaction of chlorine atoms with *i*-butanol proceeds 51 ± 5% via attack on the α-position to give an α-hydroxy alkyl radical that reacts with O_2 to give *i*-butyraldehyde. The atmospheric fate of $(CH_3)_2C(O)CH_2OH$ alkoxy radicals is decomposition to acetone and CH_2OH radicals. The atmospheric fate of $OCH_2(CH_3)CHCH_2OH$ alkoxy radicals is decomposition to formaldehyde and CH_3CHCH_2OH radicals. The results are consistent with, and serve to validate, the mechanism that has been assumed in the estimation of the photochemical ozone creation potential of *i*-butanol.

1. Introduction

Recognition of the importance of energy security and climate change has led to growing interest in the use of biofuels in transportation. Biofuels are typically used in blends with diesel or gasoline. The Renewable Fuel Standard established by the Energy Independence and Security Act in 2007 in the U.S. mandates the use of 36 billion gallons (136 billion liters) of renewable fuel by 2022. This corresponds to replacement of approximately 17% of the projected gasoline use for light-duty vehicles in 2022.[1] In Europe, the Renewable Energy Directive calls for use of 10% renewable energy in the transportation sector by 2020.[2]

To reduce competition with food crops and to increase the yields per hectare, research is focusing on the development of second-generation biofuels. Second-generation alcohol biofuels can be produced from biomass via either biotic routes[3] (e.g., pretreatment of cellulose and hemicellulose to release sugars that can be fermented to give ethanol, butanol, or higher alcohols) or abiotic routes[4] (e.g., gasification followed by thermochemical synthesis giving a mixture [typically C_1-C_4] of alcohols). There is interest in the use of *i*-butanol as a second generation biofuel. The chemical and physical properties of *i*-butanol are similar to those of gasoline. Unlike smaller alcohols such as ethanol, modest amounts (5−20%) of *i*-butanol can be blended into gasoline without substantially changing the energy density, water-induced phase separation performance, or volatility of the fuel blend.[5−7]

The use of alcohol biofuels will result in their release into the atmosphere. In the atmosphere, alcohols undergo photochemical oxidation initiated by the OH radical. Prior to the large scale use of alcohols, an assessment of their atmospheric chemistry and environmental impact is needed. There is a substantial kinetic and mechanistic database for smaller alcohols such as methanol, ethanol, and propanol and the atmospheric chemistry of these compounds is well understood.[8] The kinetic and mechanistic database for larger alcohols is sparse and the details of their atmospheric oxidation are unclear. There have been two studies of the kinetics of the reaction of OH radicals with *i*-butanol[9,10] and one study of the kinetics of the reaction of chlorine atoms with *i*-butanol.[9] The mechanism of the atmospheric degradation of *i*-butanol has yet to be studied. To improve our understanding of the atmospheric chemistry of alcohols, we conducted a study of the kinetics and the oxidation mechanism of *i*-butanol initiated by chlorine atoms and OH radicals.

2. Experimental Section

Experiments were performed in a 140 L Pyrex reactor interfaced to a Mattson Sirius 100 FTIR spectrometer.[11] The reactor was surrounded by 22 fluorescent blacklamps (GE F40T12BLB), which were used to photochemically initiate the experiments. Chlorine atoms were produced by photolysis of molecular chlorine.

$$Cl_2 + h\nu \rightarrow Cl + Cl \quad (1)$$

OH radicals were produced by photolysis of CH_3ONO in air.

$$CH_3ONO + h\nu \rightarrow CH_3O + NO \quad (2)$$

* To whom correspondence should be addressed. E-mail: twalling@ford.com.
[†] University of Copenhagen.
[‡] Ford Motor Company.

10.1021/jp107950d
Published on Web 11/04/2010

$$CH_3O + O_2 \rightarrow HO_2 + HCHO \quad (3)$$

$$HO_2 + NO \rightarrow OH + NO_2 \quad (4)$$

Relative rate techniques were used to measure the rate constant of interest relative to a reference reaction whose rate constant has been established previously. The relative rate method is a well established technique for measuring the reactivity of Cl atoms and OH radicals with organic compounds. Kinetic data were derived by monitoring the loss of *i*-butanol relative to one or more reference compounds. The method assumes that the reaction under investigation is the only significant loss process for the reactant and reference. The following relation is then valid:

$$\ln\left(\frac{[i\text{-butanol}]_{t_0}}{[i\text{-butanol}]_t}\right) = \frac{k_{\text{reactant}}}{k_{\text{reference}}} \ln\left(\frac{[\text{reference}]_{t_0}}{[\text{reference}]_t}\right) \quad (\text{I})$$

where $[i\text{-butanol}]_{to}$, $[i\text{-butanol}]_t$, $[\text{reference}]_{t_0}$ and $[\text{reference}]_t$ are the concentrations of *i*-butanol and the reference compound at times t_0 and t, and $k_{i\text{-butanol}}$ and $k_{\text{reference}}$ are the rate constants for reactions of Cl atoms, or OH radicals, with *i*-butanol and the reference compound. Plots of $\ln([i\text{-butanol}]_{t_0}/[i\text{-butanol}]_t)$ versus $\ln([\text{reference}]_{t_0}/[\text{reference}]_t)$ should be linear, pass through the origin, and have a slope of $k_{i\text{-butanol}}/k_{\text{reference}}$. Unless stated otherwise, quoted uncertainties represent the precision of the measurements and include two standard deviations from the regression analyses and uncertainties in the IR analysis (typically ±1−2% of the initial reactant concentrations).

CH_3ONO was synthesized by the dropwise addition of concentrated sulphuric acid to a saturated solution of $NaNO_2$ in methanol. *i*-Butanol and *i*-butyraldehyde were obtained from Sigma-Aldrich at purities of >99.5% and >99%, respectively. Experiments were conducted in 700 Torr total pressure of high purity O_2/N_2 diluent at 296 ± 2 K. Concentrations of reactants and products were monitored by FTIR spectroscopy. IR spectra were derived from 32 coadded interferograms with a spectral resolution of 0.25 cm^{-1} and an analytical path length of 26 m. To check for unwanted loss of reactants and reference compounds via heterogeneous reactions, reaction mixtures were left to stand in the chamber for 60 min. With the exception of $(CH_3)_2CHCH(Cl)OH$, there was no observable (<2%) loss of any of the reactants or products in the present work.

3. Results and Discussion

3.1. Measurement of *k*(Cl + *i*-Butanol) and *k*(Cl + *i*-Butyraldehyde). The rates of reactions 5 and 6 were measured relative to reactions 7 and 8.

$$Cl + (CH_3)_2CHCH_2OH \rightarrow \text{products} \quad (5)$$

$$Cl + (CH_3)_2CHCHO \rightarrow \text{products} \quad (6)$$

$$Cl + c\text{-}C_6H_{12} \rightarrow \text{products} \quad (7)$$

$$Cl + C_2H_4 \rightarrow \text{products} \quad (8)$$

Reaction mixtures consisted of either 30−60 mTorr *i*-butanol or 11−15 mTorr *i*-butyraldehyde, 5−30 mTorr of either *c*-C_6H_{12} or C_2H_4, and 150−250 mTorr Cl_2 in 700 Torr of air or N_2 diluent. The loss of *i*-butanol and *i*-butyraldehyde are plotted versus the reference compounds in Figure 1. Linear least-squares analysis of the data in Figure 1 gives $k_5/k_7 = 0.61 \pm 0.07$, $k_5/k_8 = 2.24 \pm 0.16$, $k_6/k_7 = 0.42 \pm 0.02$, and $k_6/k_8 = 1.47 \pm 0.06$. Using reference rate constants (at 700 Torr total pressure) of $k_7 = 3.30 \times 10^{-10}$ [12] and $k_8 = 9.29 \times 10^{-11}$ [13] gives $k_5 = (2.02 \pm 0.23) \times 10^{-10}$, $k_5 = (2.08 \pm 0.15) \times 10^{-10}$, $k_6 = (1.38 \pm 0.07) \times 10^{-10}$, and $k_6 = (1.36 \pm 0.06) \times 10^{-10}$ cm^3 $molecule^{-1}$ s^{-1}. We cite final values that are averages of the individual determinations together with error limits that encompass the extremes of the determinations, $k_5 = (2.05 \pm 0.26) \times 10^{-10}$ and $k_6 = (1.37 \pm 0.08) \times 10^{-10}$ cm^3 $molecule^{-1}$ s^{-1}. Results from the current work are compared with previous measurements in Table 1. Our result for k_5 is in excellent agreement with that reported by Wu et al.[9] Our result for k_6 is in good agreement with those reported by Ullerstam et al.[14] and Le Crâne et al.,[15] but is approximately 25% lower than the results reported by Thévenet et al.[16]

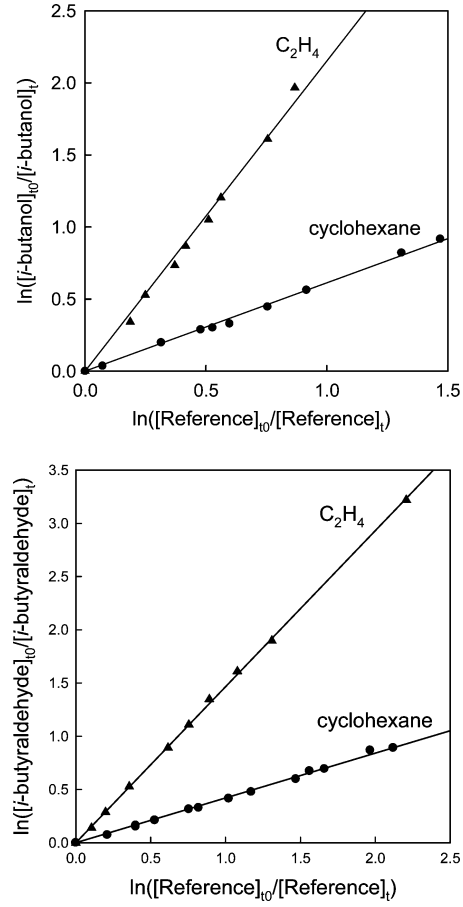

Figure 1. Loss of *i*-butanol and *i*-butyraldehyde vs ethene (triangles) and c-hexane (circles) in the presence of chlorine atoms in 700 Torr of air or N_2 at 296 ± 2 K.

3.2. Kinetics of the OH + *i*-Butanol Reaction in 700 Torr of Air. The rate of reaction 9 was measured relative to reactions 10 and 11:

$$OH + (CH_3)_2CHCH_2OH \rightarrow \text{products} \quad (9)$$

TABLE 1: Literature Data for k(Cl + *i*-Butanol) and k(Cl + *i*-Butyraldehyde)[a]

T	k(Cl + *i*-butanol)	reference	k(Cl + reference)	citation
296	2.02 ± 0.23	c-hexane	3.30	this work
296	2.10 ± 0.33	ethene	0.929	this work
295	1.94 ± 0.04	propane	1.40	Wu et al.[9]
295	2.11 ± 0.12	c-hexane	3.30	Wu et al.[9]

T	k(Cl + *i*-butyraldehyde)	reference	k(Cl + reference)	citation
296	1.38 ± 0.07	c-hexane	3.30	this work
296	1.36 ± 0.06	ethene	0.929	this work
298	1.78 ± 0.25	ethane	0.59	Thévenet et al.[16]
298	1.73 ± 0.30	propane	1.40	Thévenet et al.[16]
298	1.70 ± 0.35	*n*-butane	2.05	Thévenet et al.[16]
297	1.50 ± 0.30	propene	2.30	Ullerstam et al.[14]
298	1.38 ± 0.14	ethene	0.929	Le Crâne et al.[15]
298	1.24 ± 0.13	cyclohexane	3.30	Le Crâne et al.[15]

[a] All studies were performed using the relative rate method. Rate constants are in units of 10^{-10} cm^3 molecule^{-1} s^{-1}.

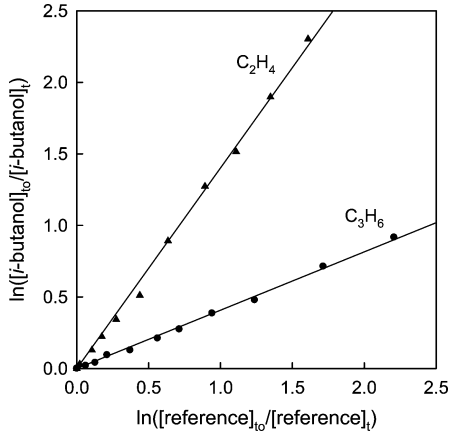

Figure 2. Loss of *i*-butanol vs ethene (triangles) and propene (circles) in the presence of OH radicals in 700 Torr of air at 296 ± 2 K.

$$OH + C_3H_6 \rightarrow \text{products} \quad (10)$$

$$OH + C_2H_4 \rightarrow \text{products} \quad (11)$$

Reaction mixtures consisted of 29−31 mTorr of *i*-butanol, 87−88 mTorr of CH_3ONO, and 7 mTorr of either C_3H_6 or C_2H_4 in 700 Torr total pressure of air diluent. Figure 2 shows the loss of *i*-butanol versus loss of the reference compounds. Linear least-squares analysis gives $k_9/k_{10} = 0.41 \pm 0.04$ and $k_9/k_{11} = 1.41 \pm 0.10$. Using reference rate constants (at 700 Torr total pressure) of $k_{10} = 2.63 \times 10^{-11}$ [17] and $k_{11} = 8.52 \times 10^{-12}$ [17] gives $k_9 = (1.08 \pm 0.11) \times 10^{-11}$ and $(1.20 \pm 0.09) \times 10^{-11}$ cm^3 molecule^{-1} s^{-1}. We cite a final value that is the average of the individual determinations together with error limits that encompass the extremes of the determinations, $k_9 = (1.14 \pm 0.17) \times 10^{-11}$ cm^3 molecule^{-1} s^{-1}. As seen from Table 2, the results from the three independent studies of k_9 are in good agreement.

Structure Activity Relationship (SAR) methods[18,19] can be used to estimate k(OH + *i*-butanol). Using the substituent factors proposed by Bethel et al.[19] and group rate constants given by Kwok et al.[18] and Bethel et al.,[19] the SAR method provides an estimate of $k_9 = 8.9 \times 10^{-12}$ cm^3 molecule^{-1} s^{-1} with 4, 57, 37, and 2% of reaction occurring via abstraction from −CH_3, −CH, −CH_2, and −OH groups, respectively. The SAR estimate of k_9 is consistent with the experimental determinations of k_9.

3.3. Mechanism of the Cl + *i*-Butanol Reaction Studied in 700 Torr of N_2. The mechanism of the reaction of Cl atoms with *i*-butanol was investigated by irradiating mixtures of 29 mTorr of *i*-butanol and 110 mTorr of Cl_2 in 700 Torr of N_2 diluent. The reaction of Cl atoms with *i*-butanol can proceed via four channels

$$Cl + (CH_3)_2CHCH_2OH \rightarrow (CH_3)_2CHCHOH + HCl \quad (5a)$$

$$Cl + (CH_3)_2CHCH_2OH \rightarrow (CH_3)_2CCH_2OH + HCl \quad (5b)$$

$$Cl + (CH_3)_2CHCH_2OH \rightarrow (CH_3)(CH_2)CHCH_2OH + HCl \quad (5c)$$

$$Cl + (CH_3)_2CHCH_2OH \rightarrow (CH_3)_2CHCH_2O + HCl \quad (5d)$$

Hydrogen abstraction from the −OH group (reaction 5d) in alcohols is endothermic by approximately 5 kJ mol^{-1} [8] and is not considered further. The radicals generated in reactions 5a−c react with molecular chlorine via reactions 12−14

$$Cl_2 + (CH_3)_2CHCHOH \rightarrow (CH_3)_2CHCH(Cl)OH + Cl \quad (12)$$

$$Cl_2 + (CH_3)_2CCH_2OH \rightarrow (CH_3)_2CClCH_2OH + Cl \quad (13)$$

$$Cl_2 + (CH_3)(CH_2)CHCH_2OH \rightarrow (CH_3)(CH_2Cl)CHCH_2OH + Cl \quad (14)$$

By analogy to the behavior of other alkyl radicals,[20] it is expected that the rate constants for reactions 12−14 will be on the order of 10^{-12} to 10^{-11} cm^3 molecule^{-1} s^{-1}. In the present experiments with 110 mTorr of Cl_2 in 700 Torr of nitrogen, reactions 12−14 will be the dominant fate of the radicals produced by reaction 5. It has been observed in previous experiments using the chamber at Ford that α-chloro-alcohols such as CH_2ClOH,[21] $CHCl_2OH$,[21] CCl_3OH,[21] $CH_3CHClOH$,[22] $CH_3CClOHCH_3$,[23] and $CH_3(CH_2)_2CHClOH$[24] decompose heterogeneously in the chamber via elimination of HCl to give the corresponding carbonyl compounds on a time scale typically of a few minutes. Similar behavior was observed in the present study with the formation of *i*-butyraldehyde (complete within 5−10 min) on allowing reaction mixtures to stand in the dark. The *i*-butyraldehyde is generated via decomposition of $(CH_3)_2CHCHClOH$ and provides a marker for reaction 5a.

$$(CH_3)_2CHCHClOH \rightarrow (CH_3)_2CHCHO + HCl \quad (15)$$

Figure 3 shows the formation of *i*-butyraldehyde versus loss of *i*-butanol following the UV irradiation of mixtures of *i*-butanol and chlorine in 700 Torr of N_2. The decrease in the yield of *i*-butyraldehyde for experiments employing high

TABLE 2: Literature Data for *k*(OH + *i*-Butanol) near Ambient Temperature[a]

T	*k*(OH + *i*-butanol)	technique[b]	reference	*k*(OH + reference)	citation
296	1.08 ± 0.11	RR	propene	2.63	this work
296	1.20 ± 0.09	RR	ethene	0.85	this work
295	0.91 ± 0.04	RR	propane	0.11	Wu et al.[9]
295	0.99 ± 0.05	RR	c-hexane	0.72	Wu et al.[9]
298	0.85 ± 0.01	RR	1-butanol	0.85	Mellouki et al.[10]
298	0.98 ± 0.01	RR	1,3-dioxalane	1.11	Mellouki et al.[10]
298	0.92 ± 0.04	PLP-LIF			Mellouki et al.[10]
296	1.05[c]	PLP-LIF			Mellouki et al.[10]

[a] Rate constants are in units of 10^{-11} cm^3 molecule^{-1} s^{-1}. [b] RR, relative rate; PLP-LIF, pulsed laser photolysis-laser induced fluorescence. [c] Average of two determinations.

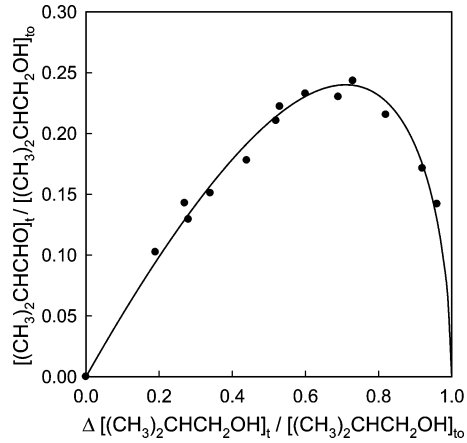

Figure 3. Formation of *i*-butyraldehyde vs loss of *i*-butanol following UV irradiation of *i*-butanol/Cl_2 mixtures in 700 Torr of nitrogen diluent.

(>60%) consumption of *i*-butanol reflects the loss of *i*-butyraldehyde via reaction with chlorine atoms. The data in Figure 3 contain information on the initial yield of *i*-butyraldehyde (which we equate to k_{5a}/k_5) and the rate constant ratio k_6/k_5. Assuming that the formation and loss of *i*-butyraldehyde are determined by reactions 5, 12, 15, and 6, then it can be shown[25] that

$$\frac{[(CH_3)_2CHCHO]_t}{[(CH_3)_2CHCH_2OH]_{t=0}} = \frac{\alpha}{1-\frac{k_6}{k_5}}(1-x)[(1-x)^{k_6/k_5-1}-1] \quad \text{(II)}$$

Where α is the yield of $(CH_3)_2CHCHO$ following reaction of chlorine atoms with $(CH_3)_2CHCH_2OH$ (k_{5a}/k_5), k_6 is the rate constant for reaction 6, and x is the fractional loss of $(CH_3)_2CHCH_2OH$ defined as:

$$x = 1 - \frac{[(CH_3)_2CHCH_2OH]_t}{[(CH_3)_2CHCH_2OH]_{t_0}} \quad \text{(III)}$$

The best fit was obtained with $\alpha = 0.53 \pm 0.03$ and $k_6/k_5 = 0.64 \pm 0.06$. Quoted errors correspond to two standard deviations from the fit. The rate constant ratio $k_6/k_5 = 0.64 \pm 0.06$ is consistent with the results reported in section 3.1; $k_6/k_7 \times k_7/k_5 = k_6/k_5 = 0.69 \pm 0.09$ and $k_6/k_8 \times k_8/k_5 = k_6/k_5 = 0.66 \pm 0.05$. From the value of α we conclude that 53 ± 3% of the reaction of chlorine atoms with *i*-butanol occurs via H-atom abstraction from the α-carbon (reaction 5a).

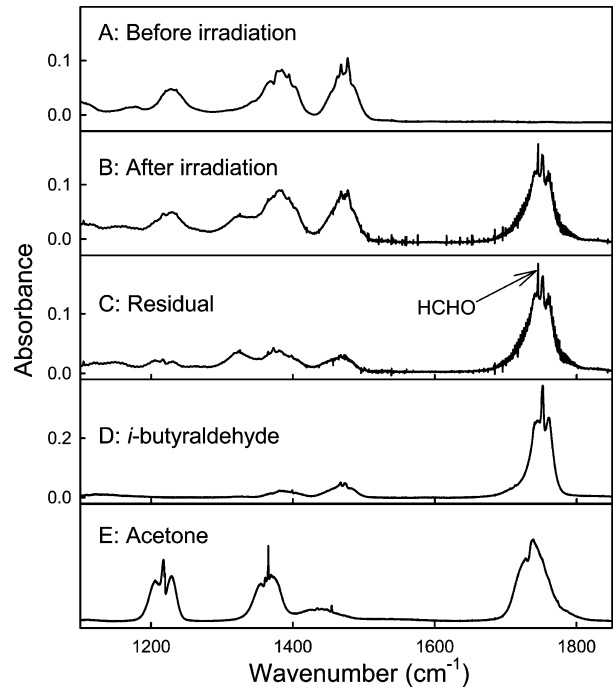

Figure 4. IR spectra obtained before (A) and after (B) 30 s of irradiation of 31 mTorr of *i*-butanol and 129 mTorr of Cl_2 in 700 Torr of air. Panel (C) is the product spectrum obtained by subtracting 65% of panel (A) from panel (B). Panels (D) and (E) are reference spectra for *i*-butyraldehyde and acetone.

3.4. Products of Cl Atom Initiated Oxidation of *i*-Butanol in 700 Torr of N_2/O_2. The mechanism of Cl atom initiated oxidation of *i*-butanol was investigated by irradiating mixtures of 30−31 mTorr of *i*-butanol, 117−1296 mTorr of Cl_2, and 15−150 Torr of oxygen in 700 Torr total pressure of N_2 diluent. Figure 4 shows spectra acquired before (A) and after (B), a 30 s irradiation of a mixture of 31 mTorr of *i*-butanol and 129 mTorr of Cl_2 in 700 Torr of air. The consumption of *i*-butanol in this experiment was 35%. Panel (C) shows the product spectrum derived by subtracting the IR features of *i*-butanol from the spectrum in panel (B). Comparison with the reference spectrum in panel (D) shows the formation of *i*-butyraldehyde.

As with other α-hydroxyalkyl radicals, reaction with O_2 giving *i*-butyraldehyde will be the sole fate of the radical generated in reaction 5a.

$$(CH_3)_2CHCHOH + O_2 \rightarrow (CH_3)_2CHCHO + HO_2 \quad \text{(16)}$$

The circles in Figure 5 show the formation of *i*-butyraldehyde versus loss of *i*-butanol observed following the UV irradiation

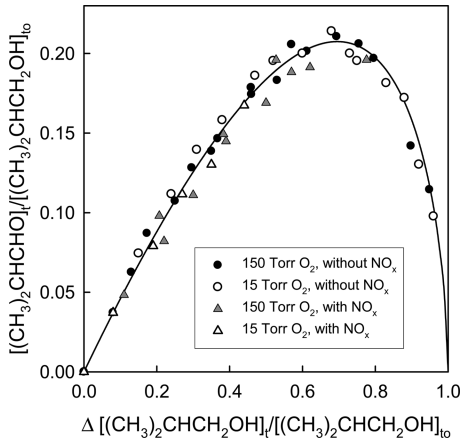

Figure 5. Formation of *i*-butyraldehyde vs the loss of *i*-butanol following UV irradiation of *i*-butanol/Cl_2 mixtures with 15 Torr of O_2 (open symbols) or 150 Torr of O_2 (closed symbols) in 700 Torr total pressure of nitrogen diluent in the presence (triangles) and absence (circles) of NO_x.

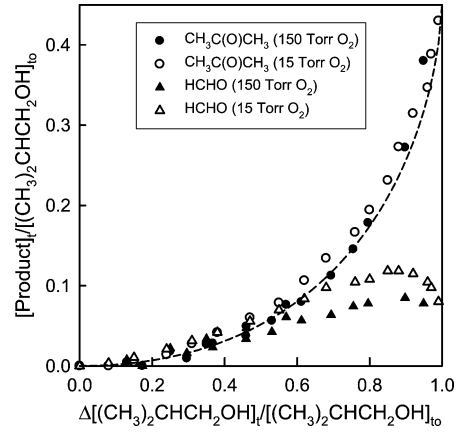

Figure 6. Formation of acetone (circles) and formaldehyde (triangles) vs the loss of *i*-butanol following UV irradiation of *i*-butanol/Cl_2 mixtures with 15 Torr of O_2 (open symbols) or 150 Torr of O_2 (closed symbols) in 700 Torr total pressure of nitrogen diluent in the absence of NO_x. The dashed line shows the expected yield of acetone based on the mechanism discussed in Section 3.4.

of *i*-butanol/Cl_2/O_2/N_2 mixtures. The filled circles are for experiments with 150 Torr O_2, open circles are for experiments with 15 Torr O_2. There was no discernible impact of [O_2] on the *i*-butyraldehyde yield. A fit of eq II to the data gives $k_6/k_5 = 0.70 \pm 0.05$ and $\alpha = 0.48 \pm 0.03$. These results are consistent with those presented in Section 3.3 obtained in 700 Torr N_2. The rate constant ratio $k_6/k_5 = 0.70 \pm 0.05$ is consistent with the results presented in Section 3.1.

As seen from comparing panels C and E in Figure 4, a small amount (0.84 mTorr) of acetone was observed. The sharp feature at 1746 cm^{-1} evident to the left of the *i*-butyraldehyde Q-branch in Figure 4C is attributable to the formation of HCHO (1.05 mTorr). Figure 6 shows the formation of acetone and formaldehyde versus the loss of *i*-butanol. Filled symbols were obtained using 150 Torr O_2, and open symbols were obtained using 15 Torr O_2. There was no discernible effect of [O_2] on the yield of acetone, but the yield of HCHO was lower in the experiment using higher [O_2]. For small consumptions (<20%) of *i*-butanol there was little, or no, formation of either acetone or HCHO, and we conclude that these compounds are not major primary products (yields <5%). For *i*-butanol consumptions of 20−60% there was a substantial increase in the observed yield of acetone and HCHO, and we conclude that these compounds are formed as secondary products. For *i*-butanol consumptions of >60% the yield of HCHO reaches a maximum and then declines; in contrast, the yield of acetone continues to increase with *i*-butanol consumption. Acetone is relatively unreactive towards chlorine atoms (k(Cl + acetone) = 2.2×10^{-12} [8]), whereas HCHO is reactive k(Cl + HCHO) = 7.2×10^{-11}.[8] The acetone yield for *i*-butanol consumptions >90% tends towards a value that is similar to the initial *i*-butyraldehyde yield (see previous sections). The simplest explanation for the acetone formation shown in Figure 6 is that it is formed via chlorine-initiated oxidation of *i*-butyraldehyde:

$$(CH_3)_2CHCHO + Cl \rightarrow (CH_3)_2CHCO + HCl \quad (6a)$$

$$(CH_3)_2CHCO + O_2 \rightarrow (CH_3)_2CHC(O)O_2 \quad (17)$$

$$(CH_3)_2CHC(O)O_2 + RO_2 \rightarrow (CH_3)_2CHC(O)O + RO + O_2 \quad (18)$$

$$(CH_3)_2CHC(O)O \rightarrow (CH_3)_2CH + CO_2 \quad (19)$$

$$(CH_3)_2CH + O_2 \rightarrow (CH_3)_2CHO_2 \quad (20)$$

$$(CH_3)_2CHO_2 + RO_2 \rightarrow (CH_3)_2CHO + RO + O_2 \quad (21)$$

$$(CH_3)_2CHO + O_2 \rightarrow CH_3C(O)CH_3 + HO_2 \quad (22)$$

The dashed curve in Figure 6 shows the expected yield of acetone based on the values of $k_6/k_5 = 0.70 \pm 0.05$ and $\alpha = 0.48 \pm 0.03$ (see above) and $k_{6a}/k_6 = 0.85$.[15] As seen from Figure 6, the observed formation of acetone is consistent with its formation as a secondary product following reaction of chlorine with *i*-butyraldehyde. In contrast to the situation for acetone, there are several potential secondary reactions that could give HCHO in the system and it is difficult to point to a precise source.

We attribute the absence of acetone and formaldehyde as observable primary products in the experiments performed in the absence of NO_x to significant loss of $(CH_3)_2C(OO)CH_2OH$ peroxy radicals via reactions with HO_2 and other peroxy radicals in reactions that do not lead to the formation of the alkoxy radical. For example,

$$(CH_3)_2C(OO)CH_2OH + HO_2 \rightarrow (CH_3)_2C(OOH)CH_2OH + O_2 \quad (23)$$

The relative importance of reaction 23 probably reflects a very slow rate of self-reaction of $(CH_3)_2C(OO)CH_2OH$ radicals which would be consistent with the slow rate of self-reaction of $(CH_3)_3COO$ radicals.[26]

3.5. Products of Cl Atom Initiated Oxidation of *i*-Butanol in the Presence of NO in 700 Torr of N_2/O_2. The mechanism of chlorine atom initiated oxidation of *i*-butanol in the presence of NO was investigated by irradiating mixtures of 29−30 mTorr *i*-butanol, 118−225 mTorr Cl_2, 59−76 mTorr NO, and 15−150

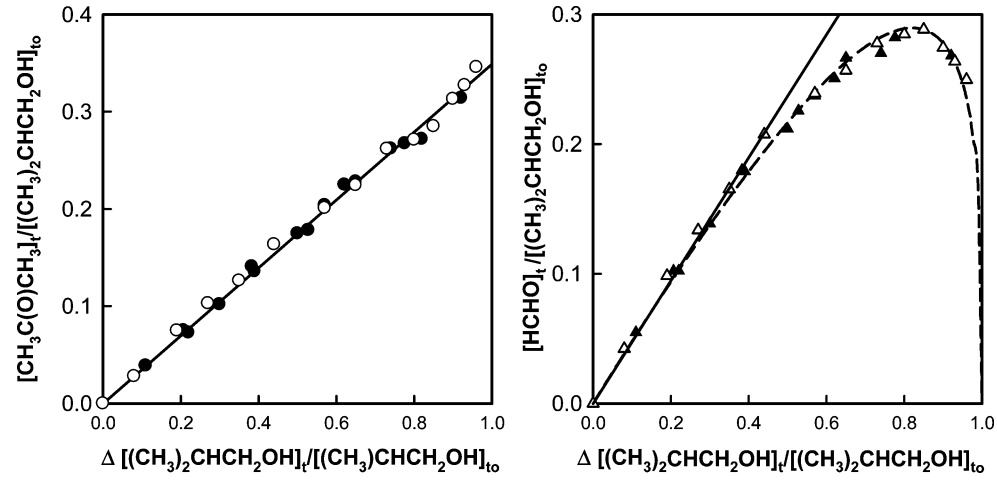

Figure 7. Formation of acetone(circles) and formaldehyde (triangles) vs the loss of *i*-butanol following UV irradiation of *i*-butanol/Cl_2 mixtures with 15 Torr of O_2 (open symbols) or 150 Torr of O_2 (closed symbols) in 700 Torr total pressure of nitrogen diluent in the presence of NO_x. The solid lines are least-squares fits. The dashed line is a fit of an expression analogous to expression II, see Section 3.5.

Torr oxygen in 700 Torr of nitrogen. The observed products were *i*-butyraldehyde, formaldehyde, and acetone. The presence of NO ensures rapid removal of RO_2 (converted into RO radicals and, to a small degree, organic nitrates, $RONO_2$) and HO_2 radicals (converted into OH radicals).

$$RO_2 + NO \rightarrow RO + NO_2 \quad (24a)$$

$$RO_2 + NO + M \rightarrow RONO_2 + M \quad (24b)$$

$$HO_2 + NO \rightarrow OH + NO_2 \quad (25)$$

The presence of NO simplifies the mechanistic interpretation of the product yields because it provides a more direct conversion of peroxy into alkoxy radicals via reaction 24a and removes the need to consider $RO_2 + RO_2$ and $RO_2 + HO_2$ reactions. As discussed in Section 4, the formation of OH radicals does not appear to have a major impact on the chemistry in these experiments.

The triangles in Figure 5 show the formation of *i*-butyraldehyde in the presence of NO. There was no discernible effect of $[O_2]$ over the range studied and the yield of *i*-butyraldehyde observed in the presence of NO_x was indistinguishable from that in the absence of NO_x. This behavior is consistent with reaction 16 being the source of *i*-butyraldehyde; NO is not expected to compete with O_2 for the available α-hydroxy alkyl radicals. Fitting expression II to the NO_x data in Figure 5 gave an initial *i*-butyraldehyde yield of 46 ± 3%.

Figure 7 shows the formation of formaldehyde and acetone versus loss of *i*-butanol. Filled symbols are data obtained with 150 Torr of O_2 and open symbols were obtained with 15 Torr of O_2. There was no discernible impact of $[O_2]$ on the product yields. In marked contrast to the experiments performed in the absence of NO (see Figure 6), both acetone and formaldehyde are observed as primary products. The lines through the data in Figure 7 are linear least-squares fits (for consumptions of *i*-butanol <40% in the case of HCHO) and give molar yields of 35 ± 3% and 49 ± 3% for acetone and formaldehyde, respectively. The dashed line through the HCHO data is a fit of an equation analogous to that given in expression II. This fit is provided as a guide for visual inspection of the data trend, because the source of the HCHO is unclear we are not able to derive kinetic data from the plot.

Formaldehyde and acetone can be generated by decomposition of the hydroxyalkoxy radical generated by H-abstraction from the β-carbon atom, via reactions 26, 27 and 28. The reaction sequence will result in the formation of equal amounts of acetone and formaldehyde. Since no $CH_3C(O)CH_2OH$ was observed (yield <5%), reaction 29 can be excluded. The formation of acetone serves as a marker for reaction 5b and the acetone yield provides a value of $k_{5b}/k_5 = 0.35 \pm 0.03$.

$$(CH_3)_2CCH_2OH + O_2 \rightarrow (CH_3)_2C(O_2)CH_2OH \quad (26)$$

$$(CH_3)_2C(O_2)CH_2OH + NO \rightarrow (CH_3)_2C(O)CH_2OH + NO_2 \quad (27)$$

$$(CH_3)_2C(O)CH_2OH \rightarrow CH_3C(O)CH_3 + CH_2OH \quad (28)$$

$$(CH_3)_2C(O)CH_2OH \rightarrow CH_3C(O)CH_2OH + CH_3 \quad (29)$$

The yield of formaldehyde exceeds that of acetone by 14 ± 6% and probably reflects the chemistry associated with H-abstraction from the γ -carbon atom indicated in the scheme in Figure 8. Hydrogen abstraction from the γ-carbon atom in *i*-butanol followed by oxygen addition and reaction with NO forms the γ-hydroxyalkoxy radical which can then decompose to formaldehyde and CH_3CHCH_2OH. The reaction sequence is similar to reactions 26−28 for the β-hydroxyalkoxy radical, and it provides an explanation for the additional formaldehyde formation. The β-hydroxyalkyl radical formed by decomposition of $(CH_3)(CH_2O)CHCH_2OH$ will react further with O_2 and NO to form the β-hydroxyalkoxy radical, $CH_3CH(O)CH_2OH$. The same alkoxy radical is formed in the oxidation of *n*-propanol and is known to decompose[27] to give CH_3CHO and a CH_2OH radical, which then reacts with O_2 to give another molecule of formaldehyde.

$$CH_3CH(O)CH_2OH \rightarrow CH_3CHO + CH_2OH \quad (30)$$

As shown in the scheme in Figure 8, the γ-hydroxyalkoxy radical leads to the formation of two formaldehyde molecules.

As noted above, the absence of an effect of $[O_2]$ on the HCHO yield shown in Figure 7 indicates that reaction with O_2 does not compete with decomposition as a fate of $(CH_3)(CH_2O)CHCH_2OH$ radicals. Geiger et al.[28] have reported that reaction with O_2 and decomposition are competing fates for the structurally similar isobutoxy radical, $(CH_3)(CH_2O)CHCH_3$. Further work is needed to better understand the behavior of these alkoxy radicals.

3.6. Products of OH Radical Initiated Oxidation of *i*-Butanol in 700 Torr of Air. The products of OH radical initiated oxidation of *i*-butanol in the presence of NO were investigated by irradiating mixtures of 27−28 mTorr of *i*-butanol, 125−132 mTorr of CH_3ONO and 0−13 mTorr of NO in 700 Torr air diluent. Acetone was observed as a major product. The formation of acetone is plotted versus loss of *i*-butanol in Figure 9. The line through the data is a linear least-squares fit that gives an acetone yield of 61 ± 4%. We looked for IR features attributable to *i*-butyraldehyde in the product spectra, but absorption by CH_3ONO and its photolysis products precluded the detection of *i*-butyraldehyde. The observation of acetone in a yield of 61 ± 4% is consistent with expectations based upon the SAR estimates (see Section 3.2) that 57% of the reaction of OH radicals with *i*-butanol occurs at the β-position and the conclusion (see Section 3.2) that decomposition via reaction 28 is the fate of $(CH_3)_2C(O)CH_2OH$ alkoxy radicals.

4. Implications for Atmospheric Chemistry

We report a large body of self-consistent data concerning the kinetics and mechanism of the oxidation of *i*-butanol. The kinetic data for reactions of Cl atoms and OH radicals reported here are consistent with the results from previous studies, and we conclude that the rates of reaction of chlorine atoms and OH radicals with *i*-butanol at ambient temperature are well established. The present work is the first study of the mechanism of the reaction of chlorine atoms with *i*-butanol. Taking an average of the *i*-butyraldehyde yields determined in N_2 discussed in Section 3.3 and in N_2/O_2 diluent in the absence of NO (and hence OH radicals) discussed in Section 3.4, we quote a final value of $k_{5a}/k_5 = 0.51 \pm 0.05$. From the yield of acetone observed in N_2/O_2 diluent in the presence of NO we derive an estimate of $k_{5b}/k_5 = 0.35 \pm 0.03$. Given that OH radicals will be formed in experiments conducted in the presence of NO, some fraction of the observed *i*-butanol loss will be attributable to reaction with OH, which would lead to an overestimation of k_{5b}/k_5. Although the fact that the presence of NO does not have a discernible impact on the *i*-butyraldehyde yield (see Figure 5) suggests that OH radicals do not make a major contribution to chemistry in the system, we opt to cite an upper limit of $k_{5b}/k_5 < 0.38$.

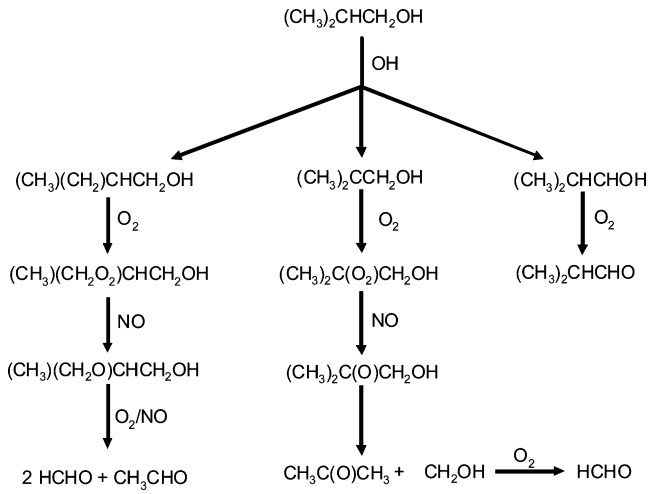

Figure 8. Mechanism of the OH-initiated oxidation of *i*-butanol.

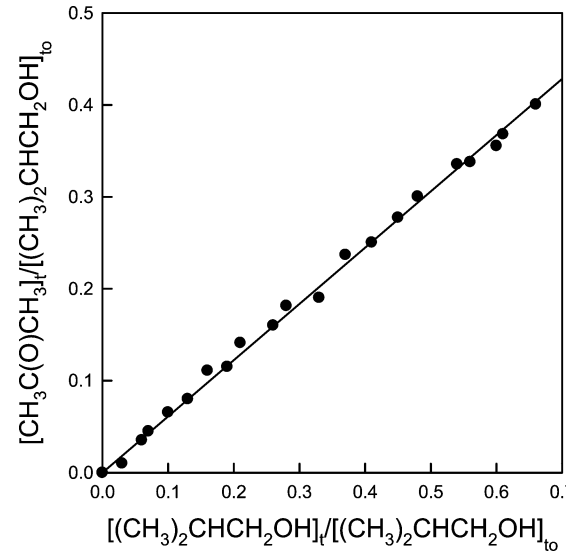

Figure 9. Formation of acetone vs the loss of *i*-butanol following UV irradiation of *i*-butanol/CH_3ONO/NO mixtures in 700 Torr of air diluent.

We report the results of the first product study of the OH radical initiated oxidation of *i*-butanol. From the observed yield of acetone we conclude that 61 ± 4% of the reaction of OH radicals with *i*-butanol occurs at the β- position. This branching ratio is indistinguishable from values estimated using SAR methods that have been used in calculations of the photochemical ozone creation potential (POCP) of *i*-butanol (e.g., by Jenkin and Hayman[29]). As indicated by the SAR calculation in Section 3.2, most of the remaining reaction is likely to proceed at the $-CH_2-$ group. The present work provides experimental validation of the *i*-butanol mechanism used in such POCP calculations. The atmospheric chemistry of *i*-butanol appears to be well established.

Acknowledgment. V. F. A. and O. J. N. acknowledge financial support from the Danish National Science Research Council, the Villum Kann Rasmussen Foundation and EUROCHAMP2.

References and Notes

(1) Anderson, J. E.; Baker, R. E.; Hardigan, P. J.; Ginder, J. M. ; Wallington, T. J. Energy Independence and Security Act of 2007: Implications for the US Light-Duty Vehicle Fleet; Society of Automotive Engineers Technical Paper, 09FFL-0302; Society of Automotive Engineers: 2009.

(2) Directive 2009/28/EC of The European Parliament and of the Council, 2009, Official Journal of the European Union, L 140/16, 2009.

(3) Farrell, A. E.; Plevin, R. J.; Turner, B. T.; Jones, A. D.; O'Hare, M.; Kammen, D. M. *Science* **2006**, *311*, 506.

(4) Atsumi, S.; Hanai, T.; Liao, J. C. *Nature* **2008**, *451*, 7174.

(5) Mueller, S. A.; Anderson, J. E.; Wallington, T. J.; Hammond, R. M. *J. Chem. Educ.* **2009**, *86*, 1045.

(6) Andersen, V. F.; Anderson, J. E.; Wallington, T. J.; Mueller, S. A.; Nielsen, O. J. *Energy Fuels* **2010**, *24*, 2683.

(7) Andersen, V. F.; Anderson, J. E.; Wallington, T. J.; Mueller, S. A.; Nielsen, O. J. *Energy Fuels* **2010**, *24*, 3647.

(8) Atkinson, R.; Baulch, D. L.; Cox, R. A.; Crowley, J. N.; Hampson, R. F.; Hynes, R. G.; Jenkin, M. E.; Rossi, M. J.; Troe, J. *Atmos. Chem.*

Phys. **2006**, *6*, 3625; IUPAC Subcommittee for Gas Kinetic Data Evaluation, http://www.iupac-kinetic.ch.cam.ac.uk.

(9) Wu, H.; Mu, Y.; Zhang, X.; Jiang, G. *Int. J. Chem. Kinet.* **2003**, *35*, 81–87.

(10) Mellouki, A.; Oussar, F.; Lun, X.; Chakir, A. *Phys. Chem. Chem. Phys.* **2004**, *6*, 2951.

(11) Wallington, T. J.; Gierczak, C. A.; Ball, J. C.; Japar, S. M. *Int. J. Chem. Kinet.* **1989**, *21*, 1077.

(12) Calvert, J. G.; Derwent, R. G.; Orlando, J. J.; Tyndall, G. S.; Wallington, T. J. *Mechanisms of Atmospheric Oxidation of the Alkanes*; Oxford University Press: 2008.

(13) Wallington, T. J.; Andino, J. M.; Lorkovic, I. M.; Kaiser, E. W.; Marston, G. *J. Phys. Chem.* **1990**, *94*, 3644.

(14) Ullerstam, M.; Ljungström, E.; Langer, S. *Phys. Chem. Chem. Phys.* **2001**, *3*, 986.

(15) Le Crâne, J.-P.; Villenave, E.; Hurley, M. D.; Wallington, T. J.; Nishida, S.; Takahashi, K.; Matsumi, Y. *J. Phys. Chem. A* **2004**, *108*, 795.

(16) Thévenet, R.; Mellouki, A.; Le Bras, G. *Int. J. Chem. Kinet.* **2000**, *32*, 676.

(17) Calvert, J. G.; Atkinson, R.; Kerr, J. A.; Madronich, S.; Moortgat, G. K.; Wallington, T. J.; Yarwood, G., *The Mechanisms of Atmospheric Oxidation of the Alkenes*; Oxford University Press: 2000.

(18) Kwok, E. S. C.; Atkinson, R. *Atmos. Environ.* **1995**, *29*, 1685.

(19) Bethel, H. L.; Atkinson, R.; Arey, J. *Int. J. Chem. Kinet.* **2001**, *33*, 310.

(20) National Institute of Standards and Technology. Standard Reference Database 17, Version 7.0, Release 1.5; http://kinetics.nist.gov/kinetics/, downloaded October 2010.

(21) Wallington, T. J.; Schneider, W. F.; Barnes, I.; Becker, K. H.; Sehested, J.; Nielsen, O. J. *Chem. Phys. Lett.* **2000**, *322*, 97.

(22) Taatjes, C. A.; Christensen, L. K.; Hurley, M. D.; Wallington, T. J. *J. Phys. Chem. A* **1999**, *103*, 9805.

(23) Yamanaka, T.; Kawasaki, M.; Hurley, M. D.; Wallington, T. J.; Schneider, W. F. *Phys. Chem. Chem. Phys.* **2007**, *9*, 4211.

(24) Hurley, M. D.; Wallington, T. J.; Laursen, L.; Javadi, M. S.; Nielsen, O. J.; Yamanaka, T.; Kawasaki, M. *J. Phys. Chem. A* **2009**, *113*, 7011.

(25) Meagher, R. J.; McIntosh, M. E.; Hurley, M. D.; Wallington, T. J. *Int. J. Chem. Kinet.* **1997**, *29*, 619.

(26) Wallington, T. J.; Dagaut, P.; Kurylo, M. J. *Chem. Rev.* **1992**, *92*, 667.

(27) Orlando, J. J.; Tyndall, G. S.; Wallington, T. J. *Chem. Rev.* **2003**, *103*, 4657.

(28) Geiger, H.; Barnes, I.; Becker, K. H.; Bohn, B.; Brauers, T.; Donner, B.; Dorn, H.-P.; Elend, M.; Freitas Dinis, C.; Grossmann, D.; Hass, H.; Hein, H.; Hoffmann, A.; Hoppe, L.; Hülsemann, F.; Kley, D.; Klotz, B.; Libuda, H. G.; Maurer, T.; Mihelcic, D.; Moortgat, G. K.; Olariu, R.; Neeb, P.; Poppe, D.; Ruppert, L.; Sauer, C. G.; Shestakov, O.; Somnitz, H.; Stockwell, W. R.; Thüner, L. P.; Wahner, A.; Wiesen, P.; Zabel, F.; Zellner, R.; Zetzsch, C. *J. Atmos. Chem.* **2002**, *42*, 323.

(29) Jenkin, M. E.; Hayman, G. D. *Atmos. Environ.* **1999**, *33*, 1275.

JP107950D